**SUPPORTING INFORMATION**

# Proteolytic Assays on Quantum Dot-Modified Paper Substrates Using Simple Optical Readout Platforms

Eleonora Petryayeva and W. Russ Algar*

Department of Chemistry, University of British Columbia, 2036 Main Mall, Vancouver, British Columbia, V6T 1Z1, Canada

*To whom correspondence should be addressed. E-mail: algar@chem.ubc.ca

## 1. Detailed Experimental Methods

### 1.1 Materials and Reagents

Lipoic acid (LA, ≥99%), *N,N'*-diisopropylcarbodiimide (DIC, >98%), *N*-hydroxysuccinimide (NHS, 98%), ethylenediamine, tetramethylammonium hydroxide (TMAH) solution in methanol (25% w/v), sodium borohydride (≥98%), sodium cyanoborohydride (95%), sodium (meta)periodate (≥99%), and glutathione (GSH) were from Sigma-Aldrich (Oakville, ON, Canada). Ammonium chloride and ammonium hydroxide (30% w/w) were from Fisher Scientific (Ottawa, ON, Canada).

Trypsin (TRP) from bovine pancreas (#T1426, TPCK treated, ≥10,000 BAEE units/mg protein), α-chymotrypsin (ChT) from bovine pancreas (#C3412, TLCK treated, Type VII, ≥40 units/mg protein), trypsinogen (pTRP) from bovine pancreas (#T1143, ≥10,000 BAEE units/mg protein after activation), α-chymotrypsinogen A (pChT) from bovine pancreas (#C4879, ≥40 units/mg solid after activation), and enterokinase (EK) from porcine intestine (#E0885, ≥100 units/mg protein) were from Sigma-Aldrich. Recombinant light chain bovine enterokinase (EK, P8070S) was from New England Biolabs (Whitby, ON, Canada).

$CdSe_{1-x}S_x$/ZnS core/shell nanocrystals (dispersed in toluene) with emission maxima at 525 nm (gQD) were from Cytodiagnostics (Burlington, ON, Canada). Peptides were from Biosynthesis Inc. (Lewisville, TX, USA). Alexa Fluor 555 (A555) C2 maleimide dye was purchased from Life Technologies (Carlsbad, CA, USA). Buffers were prepared with water purified by a Barnstead Nanopure water purification system (Thermo Scientific, Ottawa, ON, Canada) and sterilized by autoclaving prior to use. Buffers included borate buffer (50 mM, pH 9.2), borate buffer (10 mM, pH 8.5, 50 mM NaCl), Tris-HCl (20 mM, pH 7.6, 50 mM NaCl, 1 mM $CaCl_2$), and HEPES (100 mM, pH 7.0).

### 1.2 Synthesis of *N*-(2-aminoethyl)-5-(1,2-dithiolan-3-yl)pentanamide

This primary amine derivative of lipoic acid was synthesized in two steps as shown in Scheme S1.

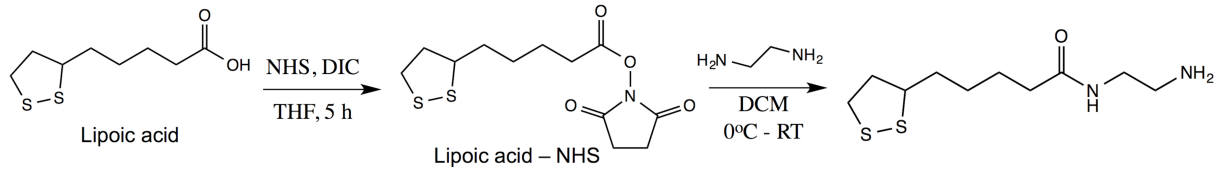


*Scheme S1.*

***Synthesis of lipoic acid-NHS.*** Lipoic acid (0.4 g, 2 mmol) and NHS (0.25 g, 2.2 mmol) were dissolved in 100 mL of anhydrous THF and cooled on ice. DIC (342 µL, 2.2 mmol) was dissolved in 20 mL of THF and added dropwise to the reaction flask. The reaction was brought to room temperature and allowed to react an additional 5 h under argon. The reaction mixture was concentrated down to 5–10 mL and 2-propanol added until turbidity (typically 50–100 mL). The reaction flask was purged with argon and placed at –20 °C overnight. The product was collected by filtration, dried, and stored at –20 °C until needed. Typical yields were 60–80%.

***Synthesis of N-(2-aminoethyl)-5-(1,2-dithiolan-3-yl)pentanamide.*** Excess ethylenediamine (10 mL, 0.15 mol) was dissolved in 10 mL of DCM and cooled on ice. Lipoic acid-NHS (0.6 g, 2 mmol) was dissolved in 50 mL of DCM, placed in an addition funnel, and added dropwise over 2 h to ethylenediamine. The reaction was brought to room temperature and allowed to react for an additional 3 h. Next, the reaction mixture was transferred to a separation funnel and washed

once with 75 mL water, three times with a solution made from 30 mL of 1 M NaOH and 20 mL of brine, and dried over sodium sulfate. The final product (LA-$NH_2$) is very prone to polymerization (decyclization and crosslinking between dithiolane rings) upon drying and was therefore stored in DCM under argon at 4 °C. Thin layer chromatography: 9:1 (v/v) DCM:MeOH, $R_f$ (LA-$NH_2$) = 0.02, $R_f$ (LA-NHS) = 0.56. TLC plates were visualized under UV light, developed with permanganate stain, and the presence of a primary amine confirmed using ninhydrin stain. $ESI^+$ MS (MeOH): m/z 249.4 ($MH^+$), 271.4 ($MNa^+$).

### 1.3 QD Ligand Exchange

Neat dihydrolipoic acid (DHLA; 100 µL) was added to organic QDs (100 µL, 10 µM) in a culture tube. The tube was sealed, purged with argon and brought to 70 °C for 2 h. The mixture was cooled briefly on ice and 200 µL of TMAH solution in methanol was added, followed by 200 µL of borate buffer (50 mM, 500 mM NaCl, pH 9.2). Approximately 1 mL of $CHCl_3$ was added to the culture tube to extract excess DHLA. The aqueous layer was transferred to 1.7 mL polypropylene centrifuge tubes in 200 µL fractions. The QDs were washed by precipitation with ethanol three times, redispersing in borate buffer (pH 9.2, 50 mM, 250 mM NaCl) between precipitation steps. After the final wash, QDs were redispersed in borate buffer (pH 9.2, 50 mM, no NaCl) and stored at 4 °C.

GSH-QDs (used for assays with EK) were prepared by diluting 100 µL (10 µM in toluene) of organic QDs with 1 mL of $CHCl_3$ and mixing with a solution of GSH (80 mg) prepared in 300 µL of TMAH in methanol. This mixture was vortexed and allowed to stand for 12 h. Subsequently, GSH-coated QDs were extracted into 200 µL of borate buffer (pH 9.2, 50 mM, 250 mM NaCl), the organic layer discarded, and QDs were precipitated with ethanol by centrifugation (4800 rcf, 4 min). QDs were redispersed in 200 µL of buffer and washed twice more with ethanol. After the final wash, QDs were dissolved in borate buffer (pH 9.2, 50 mM, no NaCl) and stored at 4 °C.

### 1.4 Peptide Labeling with Alexa Fluor 555 maleimide

Peptide with a terminal cysteine residue was labeled with Alexa Fluor 555 C2 maleimide dye according to previously published protocols with slight modifications.[1] Briefly, 0.75 mg (0.22–

0.27 μmol) of peptide was dissolved in 50 μL of 50% v/v MeCN:water, diluted with 550 μL of HEPES buffer (pH 7.0, 100 mM, 50 mM NaCl) and mixed with 0.5 mg (0.4 μmol) of A555 dye dissolved in 25 μL of DMSO. The reaction was placed on a mixer for 24 h at room temperature in the dark. Excess dye was removed using a nickel(II) nitrilotriacetic acid (Ni-NTA) agarose cartridge. The labeled peptide was desalted using an oligonucleotide purification cartridge (OPC, Life Technologies, Carlsbad, CA, USA) and quantitated using UV-visible spectrophotometry. The peptide was aliquoted into 20 nmol fractions, dried under vacuum, and stored at –20 °C until needed.

### 1.5 Instrumentation and Data Acquisition

Paper samples were illuminated with a violet (405 nm) light-emitting diode (LED; VAOL-5GUV0T4, Visual Communications Company, Poway, CA, USA). The LED was controlled and powered using LabVIEW software and a USB-6008 data acquisition (DAQ) module (National Instruments, Austin, TX, USA) unless otherwise noted. For imaging experiments with an array of spots, it was necessary to use three LEDs connected in parallel (no change in power requirements) to illuminate a sufficiently large area. In some experiments, a faint reflection of incompletely filtered LED light off the bubbles of solution on the paper substrates could be observed in images. These reflections were always away from the glowing spots of QDs, did not interfere with data analysis, and were cropped from images.

PL spectra were obtained from paper samples using a Green-Wave spectrometer (StellarNet, Tampa, FL, USA) coupled with an optical fiber (1000 μm diameter; M37L01, Thorlabs, Newton NJ, USA). A schematic of the setup is shown in Figure S1A. PL emission from a paper sample was collected using a 0.5” diameter aspheric condenser lens. A long-pass filter with a 450 nm cut-off (FEL0450, Thorlabs, Newton, NJ, USA) was placed after the lens to reject reflected light from the LED excitation source. A second lens was used to focus the collected PL emission into the optical fiber.

PL images of paper samples were acquired using either (i) a Moticam 1 (Motic Instruments, Inc., Richmond, BC, Canada) low-cost, educational-grade digital camera, (ii) a C270 webcam (Logitech, Newark, CA, USA), or (iii) an iPhone 4S (Apple, Cupertino, CA, USA). A long-pass

filter with a 500 nm cut-off (FEL0500, Thorlabs) was used to reject reflected LED light. A schematic of the setup shown in Figure S1B. Image acquisition with the Moticam 1 digital camera was done using Motic Images Plus 2.0 software (Motic Instruments). Image acquisition with the C270 webcam was done using LabVIEW software written in-house. All image analysis was done using ImageJ software (National Institutes of Health, Bethesda, MD, USA).

For characterization, confocal fluorescence images were acquired with a Leica (Concord, ON, Canada) SP5 laser scanning confocal microscope equipped with an argon laser (excitation at 458 nm, emission bandwidth 470–740 nm). Images were processed in ImageJ using the Loci plug-in. Fluorescence lifetime imaging microscopy (FLIM) was done on Zeiss LSM510 two-photon scanning confocal microscope equipped with fluorescence lifetime imaging module (Becker & Hickl GmbH, Berlin, Germany). Two-photon excitation (840 nm) was from a tunable Coherent Chameleon XR femtosecond laser. Data acquisition was done over 16 wavelength channels with an *xy*-resolution of 128 × 128 pixels and 256 time channels with data collection for 20–30 min. QD fluorescence was detected in the 525 nm channel and decay curve fitted with bi-exponential function. Solution phase PL spectra and absorbance spectra were acquired with an Infinite M1000 fluorescence plate reader (Tecan US, Inc., Morrisville, NC, USA).

$^{1}$H NMR spectra were acquired with a Bruker 400 MHz spectrometer (Bruker, Billerica, MA, USA). Electrospray ionization (ESI) mass spectra were obtained using a Waters ZQ mass spectrometer (Milford, MA, USA).

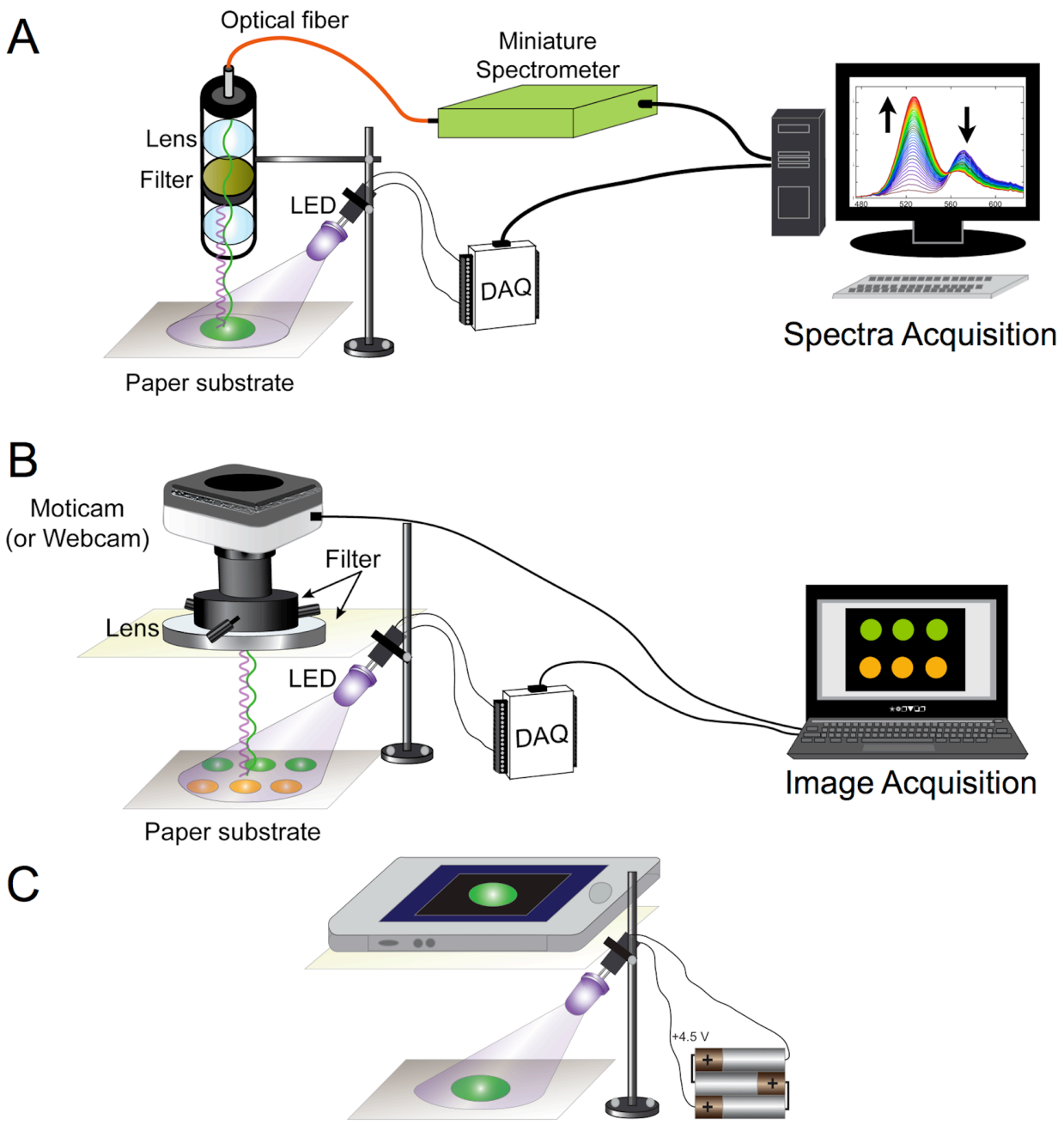


**Figure S1.** Schematics of the instrumental setups used for (A) acquisition of PL spectra, (B) color digital PL images with either a low-cost digital microscopy camera (Moticam 1) or consumer webcam, and (C) color digital PL images with a smartphone. For the smartphone imaging, the LED source was powered from three 1.5 V batteries (in series) instead of the USB connected DAQ module. Schematics are not to scale. In each case, a long-pass filter was used to block reflected LED light. The built-in color filters of the cameras discriminated between QD and dye emission.

### 1.6 Modification of Paper Substrates and Immobilization of QD-Peptide Conjugates

Chromatography paper (15–20 circular sheets, 42.5 mm, Whatman, grade 4) were oxidized in 50 mL of 50 mM sodium (meta)periodate in the dark for 1 h. Each paper sheet was washed three times with Nanopure water (Thermo Scientific, Waltham, MA, USA), once with isopropanol, and dried under vacuum. Aldehyde-functionalized paper was immersed for 12–16 h in 100 mL of dichloromethane (DCM) containing *ca.* 1 mmol of *N*-(2-aminoethyl)-5-(1,2-dithiolan-3-yl)pentanamide. Paper sheets functionalized with this lipoic acid derivative were rinsed three times with DCM, briefly air-dried, and immediately immersed into aqueous solution of sodium cyanoborohydride (50 mM) for 1 h to reduce the imine bonds to secondary amines. Paper sheets were then rinsed three times with Nanopure water, once with ethanol, dried under vacuum, and stored in the freezer. Prior to use, disulfides were reduced in 50 mM aqueous sodium borohydride solution for 2–4 h, rinsed three times with water and once with ammonium acetate buffer (100 mM, pH 4.5). The paper substrates were then dried for 5 min. QDs (1 μL of 4 μM) were spotted on the paper in an array format necessary for a particular experiment and incubated for 1 h. The paper was then rinsed in borate buffer (50 mM, pH 9.2) and excess water drained. Next, 5 μL of 50 μM A555-labeled peptide substrate was spotted and incubated for 1 h in the dark. Paper was thoroughly rinsed with borate buffer (50 mM, pH 8.5).

### 1.7 Enzyme assays

TRP and ChT protease solutions were prepared in borate buffer (10 mM, pH 8.5, 50 mM NaCl) except when used with EK. Mixtures of TRP/ChT with EK were prepared in Tris buffer (20 mM Tris, pH 7.6, 50 mM NaCl, 1 mM $CaCl_2$). Protease activity was monitored by adding 100 μL of enzyme solution to paper substrates with one spot of QD-peptide conjugates, and 200–300 μL of enzyme solution to paper substrates with two or three spots (the solution covered all spots). Inhibition assays were done with 860 nM (20 μg/mL) TRP and varying concentrations of aprotinin (0.1–15 μM). Chymotrypsinogen (pChT) was substituted for ChT and trypsinogen (pTRP) was substituted for TRP in pro-enzyme activation assays. For three-plex assays, recombinant light-chain EK was used, whereas native EK was used for activation assays. PL spectra were measured at 1 min intervals and images were acquired every 5 min for 1–2 h unless otherwise indicated.

### 1.7 Data Analysis

***FRET parameters.*** The QD-A555 FRET pair was characterized using the Förster formalism. The Förster distance, $R_\circ$ (units of cm), was calculated using Eqn. S1,

$$R_\circ^6 = 8.79 \times 10^{-28} \text{mol} \times (n^{-4} \kappa^2 \Phi_D J) \quad \text{[S1]}$$

where $n$ = 1.335 is the refractive index of the surrounding medium, $\kappa^2 = 2/3$ (assumed) is the orientation factor, $\Phi_D$ = 0.05 is the quantum yield of the donor, and $J$ is the spectral overlap, which was calculated according to Eqn. S2,

$$J = \frac{\int F_D(\lambda)\varepsilon_A(\lambda)\lambda^4 d\lambda}{\int F_D(\lambda) d\lambda} \quad \text{[S2]}$$

where $F_D$ is the fluorescence intensity of the donor and $\varepsilon_A$ is the molar absorption coefficient of the acceptor as a function of wavelength, λ. The values for $J = 6.1 \times 10^{-10}$ $\text{mol}^{-1}$ $\text{cm}^6$ and $\Phi_D = 0.05$ were calculated from experimental measurements of QDs and A555-labeled peptide in bulk solution. Fluorescein was used as a standard for quantum yield measurements.[2]

The apparent FRET efficiency, $E$, was calculated from the PL measurements using Eqns. S3, S4, and S5 as appropriate. The terms $F_D$ and $F_{DA}$ are the fluorescence intensity of the QD donors (D) in the absence and presence of A555 acceptor (A), respectively, and $<\tau_D>$ and $<\tau_{DA}>$ are the corresponding amplitude weighted PL lifetimes. $F_{AD}$ is the fluorescence intensity of the acceptor in the presence of donor. $\Phi_A = 0.09$ is the quantum yield of the A555 acceptor.

$$E = 1 - \frac{F_{DA}}{F_D} \quad \text{[S3]}$$

$$E = 1 - \frac{\langle \tau_{DA} \rangle}{\langle \tau_D \rangle} \quad \text{[S4]}$$

$$E = \frac{\Phi_D \left( \frac{F_{AD}}{F_{DA}} \right)}{\Phi_D \left( \frac{F_{AD}}{F_{DA}} \right) + \Phi_A} \qquad \text{[S5]}$$

The relationship between the A555/QD PL ratio, $F_{AD}/F_{DA}$, and FRET efficiency is defined by Eqn. S6, where $R_0$ is the Förster distance for the QD-dye FRET pair, $r$ is the QD-dye separation distance, and $n$ is the number of dye acceptors per QD donor.

$$\frac{F_{AD}}{F_{DA}} = \frac{E}{(1-E)} \left( \frac{\Phi_A}{\Phi_D} \right) = n \left( \frac{\Phi_A}{\Phi_D} \right) \left( \frac{R_0}{r} \right)^6 \qquad \text{[S6]}$$

A555/QD PL ratios were used for ratiometric data analysis and were calculated using Eqn. S7 where $\gamma = 0.022$ is the correction factor calculated as PL(568 nm)/PL(525 nm) for a sample with only QDs.

$$PL\ Ratio = \frac{PL(568\,nm) - \gamma PL(525\,nm)}{PL(525\,nm)} \qquad \text{[S7]}$$

Although Eqn. S6 strictly requires a PL ratio in terms of peak areas rather than heights, the PL ratio calculated by Eqn. S7 is still directly proportional to the right hand side of Eqn. S6, which is all that is important for the purposes of our analysis.

The R/G ratio from digital color images were calculated by splitting images into corresponding R-G-B channels, determining the mean intensity ($I$) of the spots in red (R) and green (G) channels, followed by use of Eqn. S8.

$$\frac{R}{G} ratio = \frac{\bar{I}(R)_{spot} - \bar{I}(R)_{background}}{\bar{I}(G)_{spot} - \bar{I}(G)_{background}} \qquad \text{[S8]}$$

***Normalization of progress curves.*** All experiments were done in parallel with at least one control sample with no added protease(s) to account for any drift in the LED intensity or other sources of temporal variation, including potential photobrightening or photobleaching. At each time point, $t$, either the PL ratio (Eqn. S7) or the R/G ratio (Eqn. S8), $R_{t,[E]}$, was calculated. As

shown in Eqn. S9, each of these values for a given enzyme concentration, [*E*], were normalized to an initial value of unity by dividing by the ratio at $t = 0$, and all subsequent time points were then scaled to the control sample as a reference point.

$$R_{N,t} = \frac{R_{t,[E]} \big/ R_{t=0,[E]}}{R_{t,[E]=0}} \qquad \text{[S9]}$$

***Calculation of Normalized Initial Rates.*** Normalized progress curves were fit with an exponential function in ProFit software (QuantumSoft, Bühlstr, Switzerland) using Eqn. S10. Normalized initial rates were calculated at time point, $t = 5$ min, by taking the derivative of Eqn. S10, as shown in Eqn. S11. For clarity, the normalized initial rates are reported in the text as absolute values (*i.e.*, non-negative).

$$\frac{R}{G} Ratio = 1 - a\left(1 - \exp(-bt)\right) \qquad \text{[S10]}$$

$$\frac{d}{dt}\left(\frac{R}{G} Ratio\right) = -ab\exp(-bt) \qquad \text{[S11]}$$

## 2. Additional Results and Discussion

### 2.1 LED Excitation and the QD-A555 FRET Pair

Absorption and PL spectra for QDs and A555, and the LED emission spectrum, are shown in Figure S2 (see next page). The spectral overlap integral and Förster distance for the QD-A555 FRET pair were $J = 6.1 \times 10^{-10}$ mol$^{-1}$ cm$^6$ and $R_o = 3.9$ nm, respectively. The LED intensity (input voltage = 3.3–4.5 V) was sufficient for QD excitation and no detectable direct excitation of A555 was observed.

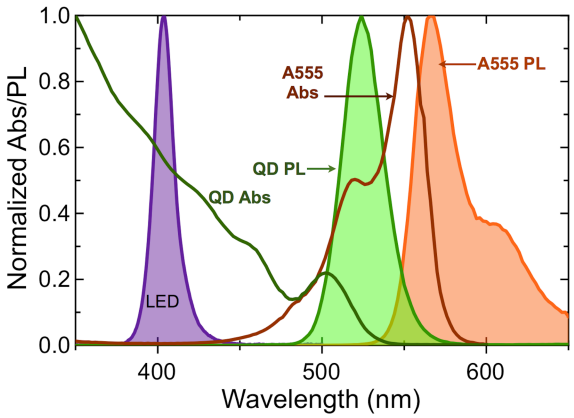


**Figure S2.** Normalized absorption and PL spectra for the QD and A555 FRET-pair. The emission profile for the LED excitation source is also shown.

## 2.2 Characterization of Paper Substrates

For the immobilization of spots of QDs on paper substrates, no change in PL intensity could be observed before and after washing, suggesting nearly quantitative immobilization. As a consequence, it was possible to estimate the number of immobilized QDs as the amount spotted. In order to estimate the amount of peptide, immobilized QDs were titrated with increasing amounts of peptide and FRET was monitored, *via* the PL ratio, up to its saturation point, as shown in Figure S3. The result was an estimated 110–115 pmol per spot of immobilized QD, or close to 30 peptides per QD.

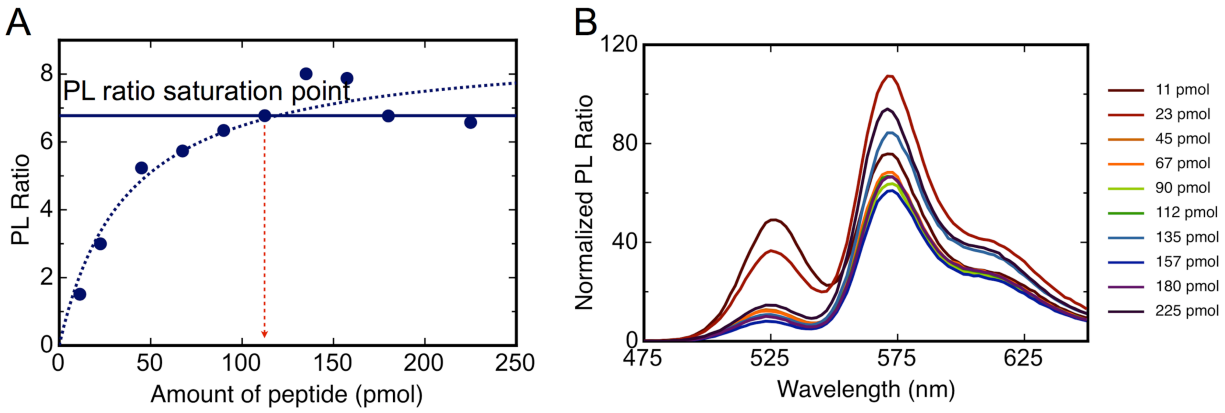


**Figure S3.** (A) Titration curve used to estimate amount of peptide conjugated to immobilized QDs. (B) PL spectra corresponding to (A).

## 2.3 Representative Raw Data from Spectrometer TRP Assay

Figure S4 shows non-normalized PL ratio data corresponding to the normalized progress curves shown in Figure 3B of the main text. Note the apparent effects of photobrightening of the QDs on the control sample (0 nM TRP).

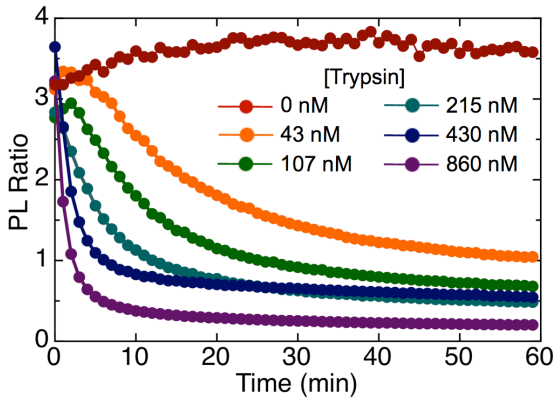


**Figure S4.** Non-normalized PL ratio progress curves for the hydrolysis of QD-Sub(TRP) conjugates catalyzed by different concentrations of TRP.

## 2.4 Trypsin Inhibition Assays with Aprotinin

Using DHLA-QDs, we carried out an inhibition assay with TRP and aprotinin, a potent competitive inhibitor of many serine proteases and a drug formerly used to control bleeding during surgical procedures.[3,4] Progress curves were obtained with 860 nM TRP at different concentrations of inhibitor (0.1, 1.0, 15 $\mu$M). Figure S5 shows R/G ratio progress curves with 860 nM TRP in the presence of different concentrations of aprotinin. In the presence of 0.1 $\mu$M aprotinin, the normalized initial rate of digestion decreased 40% from 3.18 $h^{-1}$ to 1.87 $h^{-1}$. Complete inhibition was observed at 1.0 and 15 $\mu$M aprotinin.

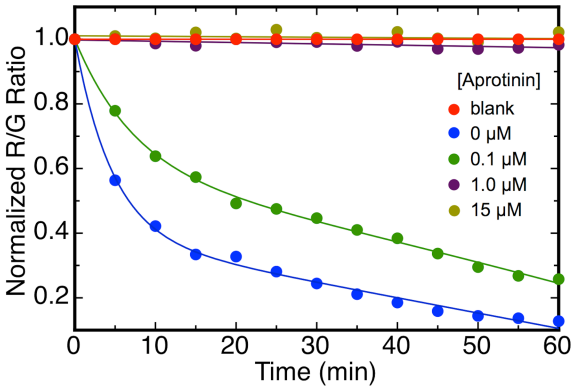


**Figure S5.** Progress curves showing the inhibition of TRP (860 nM, 20 μg/mL) activity by different concentrations of aprotinin.

### 2.5 Chymotrypsin Protease Assays

The assay format was very easily adapted to ChT by self-assembling A555-labeled Sub(ChT) peptides to a spot of immobilized QDs instead of Sub(TRP). Exposure of immobilized QD-Sub(ChT) conjugates to increasing concentrations of ChT (0–2.0 $\mu$M) resulted in progress curves with incrementally faster decreases in R/G ratio, analogous to the experiments with TRP. Figure S6A-C shows raw R/G ratios for immobilized QD-Sub(ChT) exposed to different concentrations of ChT. This data illustrates the conversion of raw data to processed data. In Figure S6D, raw R and G channel data is shown, which illustrates a small amount of non-ideal behavior typical of the paper assays with DHLA- and GSH-coated QDs. There is a small increase in the R/G ratio in the absence of protease (*i.e.,* blank sample) over the course of the assay. Such behavior, as well as variability associated with paper substrates, was observed as slight differences in R/G ratio between spots and experiments. These factors, as well as any temporal fluctuations in instrumental response, were accounted for by normalizing the data according to Eqn. S9. These progress curves were analyzed to determine normalized initial rates of digestion and an apparent $K_{m,app}$ = 145 ± 27 nM was derived (see Figure S6E). This value is slightly lower than reported for a previous assay for ChT activity with QD-peptide conjugates.[5] The LOD was 1.8 nM (0.05 $\mu$g/mL) of ChT.

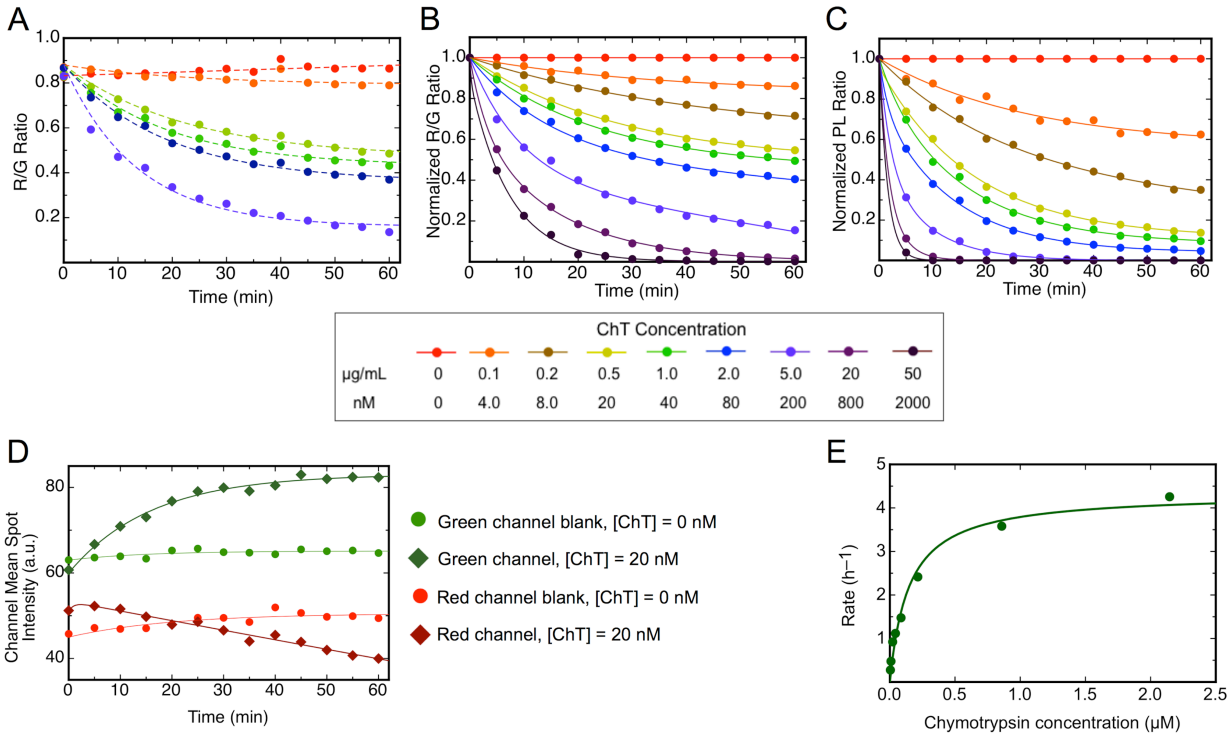


**Figure S6.** (A) Examples of raw R/G ratio progress curves obtained from color images of immobilized QD-Sub(ChT) spots upon exposure to different concentrations of ChT. (B) Normalized R/G progress curves derived from the data in panel A and additional data. (C) PL ratio progress curves derived from the data in panel B and the power relationship between R/G and PL ratios. (D) Representative examples of changes in mean intensity in the G and R channels for QD-Sub(ChT) exposed to buffer (blank) and 20 nM ChT. (E) Calibration curve for ChT activity based on normalized initial rates derived from the progress curves in panel B. The curve was used to determine the apparent $K_m$.

## 2.6 Representative Raw Data from Digital Camera TRP and ChT Assay

Figure S7A-C shows non-normalized R/G ratio data corresponding to the normalized progress curves shown in Figure 5A-C of the main text. Any effects from photobrightening are much less pronounced in this format.

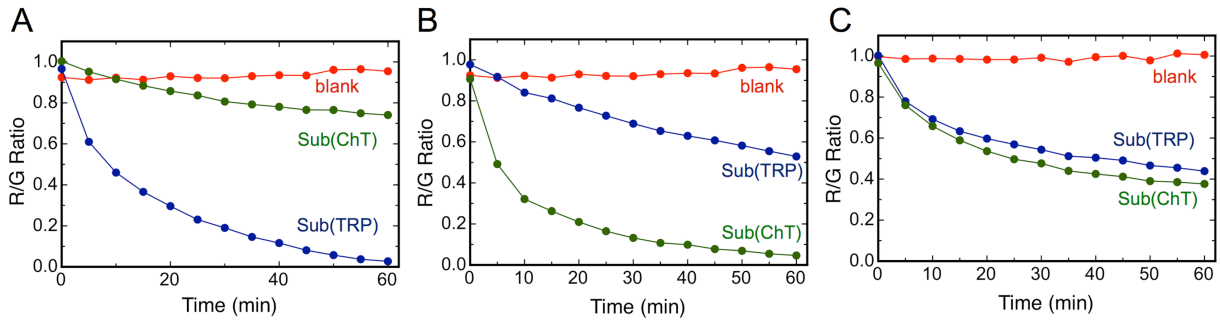


**Figure S7.** Non-normalized R/G ratio progress curves for exposure of immobilized spots of QD-Sub(TRP) and QD-Sub(ChT) to protease mixtures containing (A) 215 nM (5 μg/mL) TRP and 8 nM (0.2 μg/mL) ChT, (B) 86 nM (2 μg/mL) TRP and 80 nM (2 μg/mL) ChT, and (C) 8.6 nM (0.2 μg/mL) TRP and 200 nM (5 μg/mL) ChT. Only the negative control spot with Sub(TRP) is shown (blank). The corresponding normalized data is shown in Fig. 5.

## 2.7 Three-Plex Assay

A mixture of 7.6 nM EK, 8.6 nM TRP and 8.0 nM ChT was applied to three paper spots modified with GSH-coated QDs and either Sub(TRP), Sub(ChT), or Sub(EK). Three replicate spots were used as negative controls (blanks). Progress curves are shown in Figure S8.

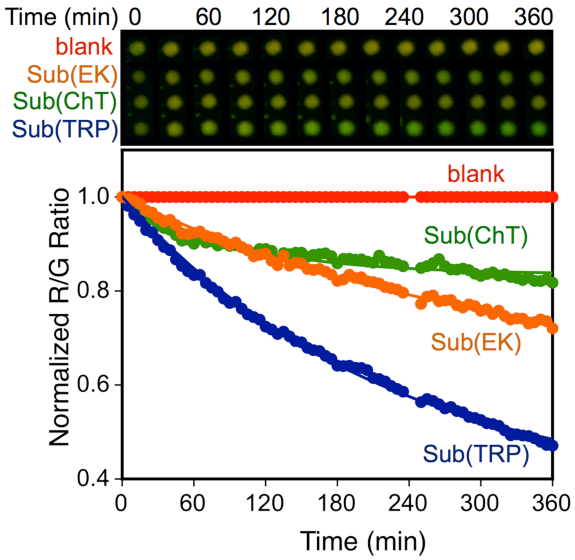


**Figure S8.** Progress curves and corresponding color digital images for multiplexed protease assays. Spots of GSH QDs functionalized with Sub(TRP), Sub(ChT), and Sub(EK) were tested against a mixture containing TRP 8.6 nM (0.2 μg/mL), ChT 8.0 nM (0.2 μg/mL), and EK 7.6 nM (0.2 μg/mL). Only the negative control spot with Sub(TRP) is shown.

## 2.8 More on Activation Assays

Initial experiments measured the direct activation of pChT by TRP (Figure 6A, step II). Progress curves for digestion of QD-Sub(TRP) and QD-Sub(ChT) upon exposure to a mixture of 215 nM (5 $\mu$g/mL) TRP and 195 nM (5 $\mu$g/mL) pChT are shown in Figure S9. As discussed in the main text, rates of digestion of Sub(ChT) were slower than in assays with initially active ChT. Note that digestion of Sub(ChT) was a function of both the activation rate of pChT and the subsequent action of ChT on Sub(ChT). An interesting observation in these paper-based activation assays was the absence of a clear lag-time and inflection in the progress curve for activated pro-ChT. In prior solution phase assays, such features were observed and attributed to the transition from pChT to ChT.[6,7] The heterogeneous kinetics of the paper assay system appears to have obscured these details, albeit that net activation was clearly observed.

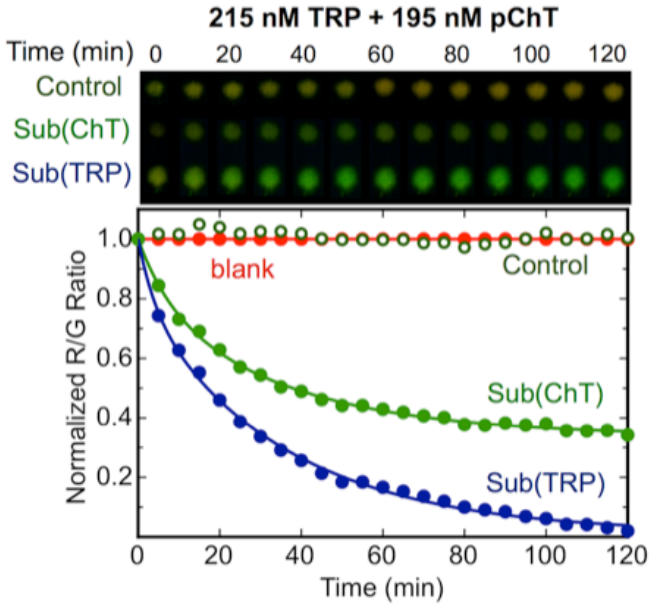


**Figure S9.** Progress curves and corresponding color digital images for direct activation of 195 nM pChT (5 µg/mL) by 215 nM TRP (5 µg/mL). Open circles correspond to the control samples containing only pChT at 5 µg/mL.

We next assayed a two-step proteolytic cascade with sequential activation of pTRP and pChT initiated by EK (Figure 6A, steps I and II). Progress curves for the digestion of Sub(TRP) and Sub(ChT) with a mixture of pTRP (210 nM, 5 $\mu$g/mL), pChT (195 nM, 5 $\mu$g/mL), and EK (5 units) are shown in Figure 6B and discussed therein. A follow-up experiment with a ten-fold reduction in the EK concentration (0.5 units) with a constant amount of pTRP and pChT resulted

in a pronounced decrease in the digestion rate of Sub(TRP) (1.0 $h^{-1}$) but had minimal effect on the digestion rate of Sub(ChT) (0.50 $h^{-1}$) as shown in Figure S10. Activation of pTRP by EK thus occurred at a much slower rate than activation of pChT by TRP.

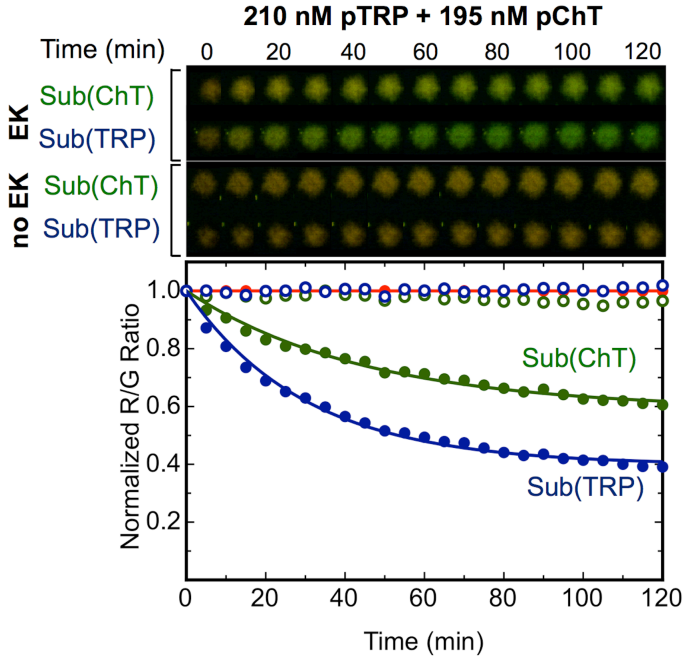


**Figure S10.** Progress curves and corresponding color digital images for cascade activation of 210 nM pTRP (5 μg/mL) and 195 nM pChT (5 μg/mL) initiated with native EK (0.5 units).

**References**


(1) Algar, W. R.; Blanco-Canosa, J. B.; Manthe, R. L.; Susumu, K.; Stewart, M. H.; Dawson, P. E.; Medintz, I. L. *Methods Mol. Biol.* **2013**, *1025*, 47-73.

(2) Grabolle, M.; Spieles, M.; Lesnyak, V.; Gaponik, N.; Eychmuller, A.; Resch-Genger, U. *Anal. Chem.* **2009**, *81*, 6285-6294.

(3) Kuepper, F.; Dangas, G.; Mueller-Chorus, A.; Kulka, P. M.; Zenz, M.; Wiebalck, A. *Blood Coagul. Fibrinolysis* **2003**, *14*, 147-153.

(4) Smith, M.; Kocher, H. M.; Hunt, B. J. *Int. J. Clin. Pract.* **2010**, *64*, 84-92.

(5) Medintz, I. L.; Clapp, A. R.; Brunel, F. M.; Tiefenbrunn, T.; Uyeda, H. T.; Chang, E. L.; Deschamps, J. R.; Dawson, P. E.; Mattoussi, H. *Nat. Mater.* **2006**, *5*, 581-589.

(6) Algar, W. R.; Ancona, M. G.; Malanoski, A. P.; Susumu, K.; Medintz, I. L. *ACS Nano* **2012**, *6*, 11044-11058.

(7) Algar, W. R.; Malanoski, A. P.; Susumu, K.; Stewart, M. H.; Hildebrandt, N.; Medintz, I. L. *Anal. Chem.* **2012**, *84*, 10136-10146.